**ICONIC 2007**
St. Louis, MO, USA
June 27-29, 2007

# FLUORESCENCE IMAGING WITH NANOMETER PRECISION USING SPECTRAL SELF-INTERFERENCE MICROSCOPY

**Brynmor J. Davis[1], P. Scott Carney[1], Anna K. Swan[2], M. Selim Ünlü[2], W. Clem Karl[2] and Bennett B. Goldberg[2]**

[1]Beckman Institute for Advanced Science and Technology
Department of Electrical and Computer Engineering
University of Illinois at Urbana-Champaign, Urbana IL, 61801, USA
E-mail: bryn@uiuc.edu

[2]Department of Electrical and Computer Engineering
Boston University, Boston MA, 02215, USA

**Abstract.** Spectral Self-Interference Fluorescence Microscopy (SSFM) has been shown to allow nanometer-scale localization of fluorescent layers placed above a reflecting substrate. A Monte-Carlo analysis is used to show how this high localization accuracy can still be expected at the low signal levels associated with single-molecule studies. Discrimination of fluorophores separated by a few tens of nanometers is also demonstrated. The results achieved indicate that SSFM may be applied to total internal reflection fluorescence microscopy to axially resolve objects within the evanescent excitation volume.

***Keywords:*** Spectral Self-Interference, Resolution, Localization, Single Molecule Imaging, Total Internal Reflection Fluorescence (TIRF) Microscopy, Fluorescence

## 1 INTRODUCTION

In both synthetic and natural objects, Spectral Self-Interference Fluorescence Microscopy [1-3] has been shown to provide highly accurate estimates of the axial location of a fluorescent layer. In SSFM a reflective surface below the object provides a second reflected path (in addition to the direct-propagation path) from the fluorophore to the detector. The interference produced by the summation of these two fields varies with the emitted wavelength and the distance from the fluorophore to the mirror. As a result, the position of the fluorophore is encoded on the spectrum measured at the detector.

This work explores the potential of using SSFM techniques in other nano-scale imaging modalities – particularly single-molecule imaging and Total Internal Reflection Fluorescence (TIRF) microscopy [4]. Recent single-molecule studies (e.g. [5]) have focused on providing three-dimensional spatial information. SSFM can provide imaging in the (usually unobserved) axial dimension provided it can be expected to work at the low signal levels associated with single-molecule observations. TIRF microscopy uses evanescent excitation to limit imaging to a very thin layer along a surface. Figure 1 shows how TIRF microscopy and SSFM can be combined into a single instrument having the potential for axial imaging within the excitation volume. The ability of SSFM to image two closely spaced fluorophores in this configuration is also investigated.

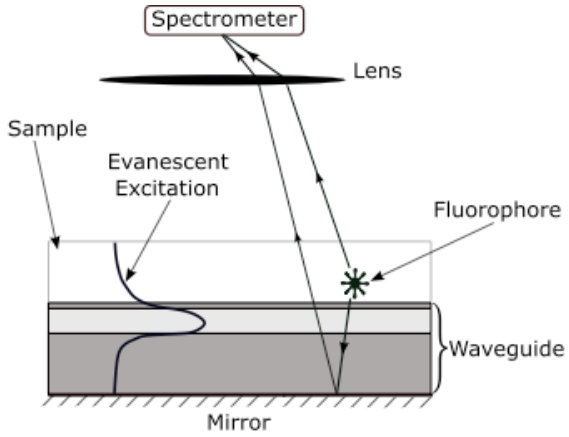


Figure 1: Illustration of an evanescently-excited spectral self-interference fluorescence microscope. Light is launched into a guiding substrate above the mirror, giving an evanescent field above the sample-substrate boundary.

## 2 SSFM IMAGE RECONSTRUCTION

Since SSFM imaging is linear, its discretized data-collection model can be represented by a matrix operator **C**, while the three-dimensional object can be mapped to a one-dimensional input vector **x**. The $i^{th}$ column of **C** then represents data resulting from the $i^{th}$ location in the object. Noise-free discrete data **y** can therefore be written as,

$$\mathbf{y} = \mathbf{C}\mathbf{x}. \tag{1}$$

The object is then estimated according to the constrained minimization procedure

$$\hat{\mathbf{x}} = \underset{\mathbf{x}}{\operatorname{argmin}} \left\| \mathbf{y} - \mathbf{C}\mathbf{x} \right\| \qquad \text{s.t.} \qquad \mathbf{x} \in \mathbf{A}. \tag{2}$$

Here **A** is the set of objects consistent with prior knowledge of the sample (e.g. the sample may be known to consist of a single fluorescent layer). The form of the norm used in (2) can be determined by applying the statistical Maximum Likelihood (ML) decision rule [6]. The significant body of literature in optimization theory (e.g. [7]) provides many algorithmic options for solving (2). The most appropriate choice will depend on the set **A**.

## 3 MONTE CARLO SIMULATIONS

Synthetic data can be generated using the model **C**. To model varying collection times or fluorophore emission rates, the data can be scaled to the appropriate signal level and then corrupted with Poisson noise to simulate measurement. Applying the reconstruction criterion given in (2) completes the simulated imaging procedure. Repeating this process with different realizations of the Poisson noise allows a Monte-Carlo characterization of the imaging performance. In this work an evanescently-excited SSFM is simulated. A numerical aperture of 0.1 is used, the fluorophores are excited at a wavelength of 488nm and the emissions are collected between 500nm and 590nm. The evanescent field is modeled by that produced by a plane wave striking a water/silicon-nitride boundary at an angle of $45^o$ (the critical angle is $40.7^o$). The difference between the direct and reflected paths to the detector corresponds to 8μm in water. Example data from this system can be seen in Fig. 2.

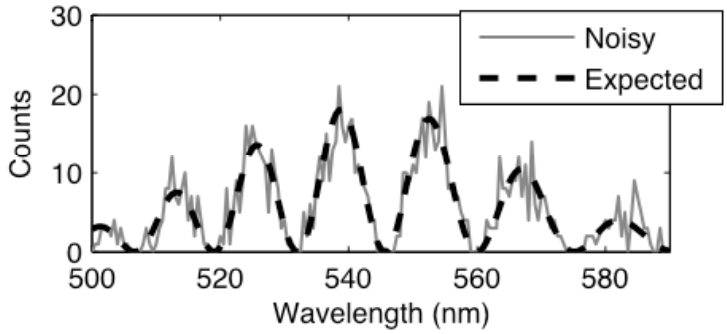


Figure 2: Simulated data from a fluorophore 20nm above the substrate boundary. The expected value of the data is shown along with an example including Poisson noise. The total expected photon count is 1000.

### 3.1 Single-structure estimation

Previous demonstrations of SSFM have imaged an object with a single axial structure and provided nanometer-scale localization information [1,2]. The instruments in those studies imaged lateral layers of fluorophores and therefore had access to a large number of photons. Motivated by single-molecule studies, the axial localization precision achieved in low-signal environments is investigated here.

The results of Monte-Carlo simulations are shown in Fig. 3. The nanometer-scale precision expected at high signal levels is seen. As the signal level is decreased, the precision of the estimate can be seen to fall, however even at very low signal levels it is still on the nanometer scale. This demonstrates SSFM's potential to provide sensitive axial localization information in single-molecule studies. Nanometer-scale precision in the lateral (i.e. perpendicular to the objective lens' optic axis) measurements can be achieved with standard imaging techniques [8] but axial measurements are less sensitive. SSFM provides a means of achieving high-precision axial localization. In addition, the evanescent excitation scheme is compatible with TIRF microscopy and its known reduction of background fluorescence noise.

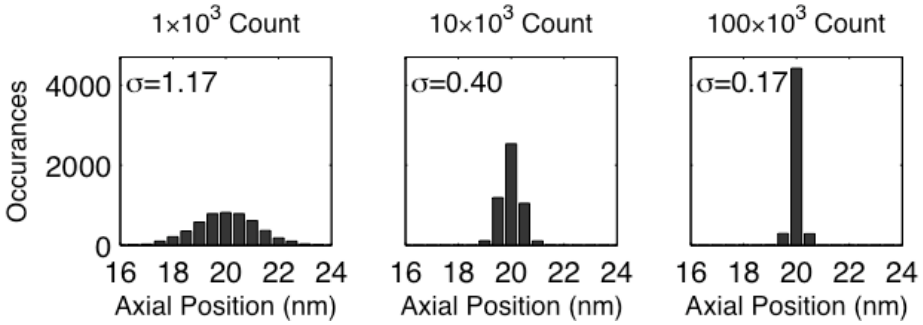


Figure 3: Histograms showing axial position estimates for a fluorophore located at 20nm. Data with total expected counts of $1\times10^3$, $10\times10^3$ and $100\times10^3$ are considered. In each case 5000 simulations were run, each with a different Poisson noise realization. The standard deviations of the estimates are inset, while the mean estimate was within 20.00±0.02nm in all cases.

### 3.2 Two-structure estimation

SSFM image reconstruction can be extended to the estimation of a two-feature object by changing the allowable image set **A** accordingly. Rather than limiting the object **x** to functions with one axial structure, it now encompasses objects with two structures. Such a case will be simulated here, with an object that is known a priori to consist of two points. This is consistent with two fluorescent molecules being present within the objective lens' focal volume.

Monte Carlo simulations showed that the data from a single SSFM measurement was not sufficient to distinguish two closely spaced fluorophores. However, if the data is augmented with a second measurement taken using a different evanescent field, the reconstruction quality is greatly improved. This phenomenon is illustrated in Fig. 4.

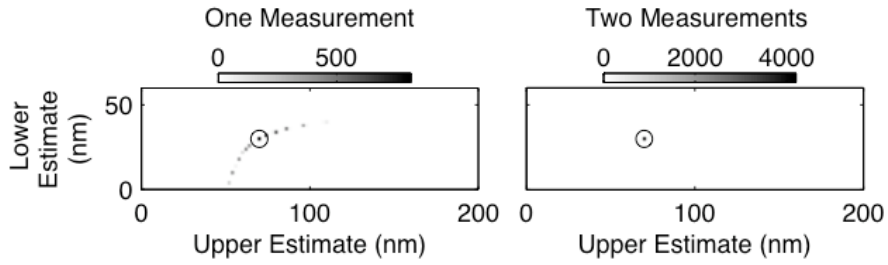


Figure 4: Two-dimensional histograms showing the estimated position pairs from data corresponding to equal strength fluorophores at 30nm and 70nm. The pixel intensity at a given point represents the number of times that position pair was estimated. The ideal position pair estimate is marked with a circle. One- (left) and two-excitation (right) cases are shown. In each case 5000 simulations were run and the total expected photon count was $200\times10^3$.

Simulations were also used to determine how the object estimate varies with signal level. The results shown in Fig. 5 show how the position estimates becomes less precise as the signal level decreases. It can be seen that at moderate signal levels, two fluorophores separated by 40nm can be distinguished. This precision is significantly lower than what can be expected for a single fluorophore as the object has become more complicated and more parameters must be estimated in order to define it. The quality of the sort of reconstruction given by (2) depends on the a priori knowledge implied by the set **A**. Such object-dependent accuracy has recently been explored in terms of lateral few-molecule imaging [9].

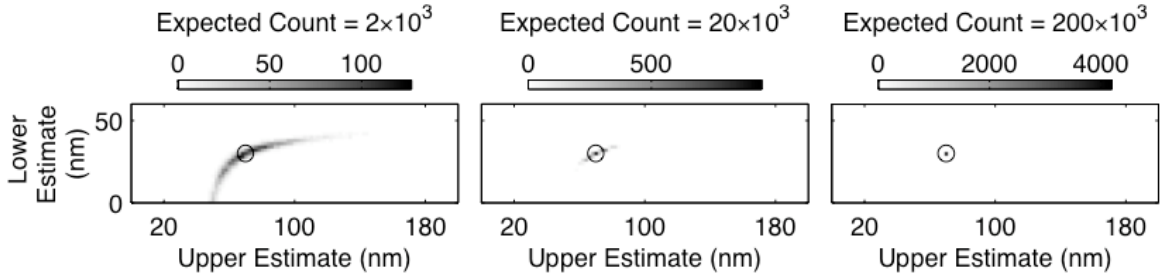


Figure 5: Two-dimensional histograms showing the estimated position pairs from data corresponding to equal strength fluorophores at 30nm and 70nm. The ideal position pair estimate is marked with a circle. Three different signal levels are considered and 5000 simulations were run in each case.

## 4 CONCLUSIONS

The capability for nanometer-scale localization of fluorescent layers using SSFM has been previously demonstrated. This study shows that the technique can be expected to produce comparable results in photon-scarce applications. In addition, SSFM can provide object information below the traditional diffraction limit when multiple fluorophores are present. These results suggest an expanded realm of applications for SSFM, including single molecule imaging and as an axial-imaging addition to TIRF microscopy.

## REFERENCES

[1] A. K. Swan, L. A. Moiseev, C. R. Cantor, B. Davis, S. B. Ippolito, W. C. Karl, B. B. Goldberg, and M. S. Ünlü, "Toward nanometer-scale resolution in fluorescence microscopy using spectral self-interference," IEEE J. Sel. Top. Quant. Electron., vol. 9, pp. 294-300, 2003.

[2] L. Moiseev, M. S. Ünlü, A. K. Swan, B. B. Goldberg, and C. R. Cantor, "DNA conformation on surfaces measured by fluorescence self-interference," Proc. Nat. Acad. Sci., vol. 103, pp. 2623- 2628, 2006.

[3] M. S. Ünlü, A. K. Swan, B. B. Goldberg, S. B. Ippolito, L. Moiseev, S. H. Lipoff and Y. Yong, "Spectral imaging for vertical sectioning," United States Patent Issued, No. 7,110,118, 19 September 2006.

[4] D. Axelrod, N. L. Thompson, and T. P. Burghart, "Total internal reflection fluorescence microscopy," J. Micros., vol. 129, pp. 19-28, 1982.

[5] E. Toprak, J. Enderlein, S. Syed, S. A. McKinney, R. G. Petschek, T. Ha, Y. E. Goldman, and P. R. Selvin, "Defocused orientation and position imaging (DOPI) of myosin V," Proc. Nat. Acad. Sci., vol. 86, pp. 6495-6499, 2006.

[6] S. M. Kay, *Fundamentals of Statistical Signal Processing: Estimation Theory.* Prentice Hall, 1993.

[7] D. P. Bertsekas, *Non-Linear Programming.* Athena Scientific, 1999.

[8] R. J. Ober, S. Ram, and E. S. Ward, "Localization accuracy in single-molecule microscopy," Biophy. J., vol. 103, pp. 1185-2000, 2004.

[9] S. Ram, E. S. Ward, and R. J. Ober, "Beyond Rayleigh's criterion: a resolution measure with application to single-molecule microscopy," Proc. Nat. Acad. Sci., vol. 103, pp. 4457-4462, 2006.